

Thermodynamic Properties of Dilute NaCl(aq) Solutions near the Critical Point of Water

Josef Sedlbauer*

Department of Chemistry, Technical University of Liberec, Halkova 6, 461 17 Liberec, Czech Republic

Robert H. Wood

Department of Chemistry and Biochemistry and Center for Molecular and Engineering Thermodynamics, University of Delaware, Newark, Delaware 19716

Received: September 17, 2003

Completely dissociated aqueous solutions of alkali halides are successfully modeled to about 500–600 K, for instance, by the ion-interaction equations. At higher temperatures, the ions associate to neutral molecules and clusters. In the more concentrated solutions, some “effective chemical continuum” treatment may be applied. Neither approach is, however, suitable for the intermediate region of near-critical temperatures and low solution concentrations, where the ions are only partially associated and thermodynamic properties are subject to rapid changes. A Helmholtz energy model coupled with chemical association was proposed for these systems and used for simultaneous correlation of experimental apparent molar volumes, apparent molar heat capacities, and association constants of dilute NaCl(aq) solutions at temperatures from 573 to 723 K and at concentrations where the solutions are partially associated. Conversion from a MacMillan–Mayer to a Lewis–Randall reference state was included in the calculations. Performance of the model for data description is good, suggesting its application for other associating electrolytes in a wide range of state conditions.

Introduction

Supercritical aqueous solutions of electrolytes are encountered in a variety of hydrothermal environments and also in technologies such as power generation or supercritical water oxidation of hazardous organic chemicals. Understanding of these phenomena largely relies on models for predicting chemical changes in the superheated water and steam. Namely, one serious and costly obstacle to industrial processes operating at elevated conditions is extensive corrosion of equipment parts (boilers, turbines, reactors, etc.) that come into contact with the solutions. The highest corrosion rates occur in the near-critical region, considered here as 573–723 K in terms of temperature. However, available models of dilute and moderately concentrated aqueous electrolyte solutions at such conditions are still inadequate for accurate prediction of their fundamental thermodynamic properties that are required for chemical equilibrium calculations. Two major problems must be taken into account when formulating a possibly successful model: strong but incomplete ionic association and anomalous behavior of the standard and excess thermodynamic properties.

Strong electrolytes completely dissociate in aqueous solutions, forming freely moving ions. This assumption is valid to about 573 K for alkali halides and provides a basis for accurate representation of solute properties by various methods, for instance, by the ion-interaction approach.^{1–3} At higher temperatures, evaluation of solute thermodynamic behavior becomes more complicated, and the main reason of this uncertainty is the unknown nature of species present in the solution. Free ions

are predominant at very low concentrations, but they tend to associate to neutral ion pairs with rising molality. Increasing the concentration further, Laria et al.⁴ suggested that at some point association reaches a maximum and redissociation of ion pairs back to single ions occurs. In contrast to that, Pitzer and Schreiber⁵ adopted an approach in which the creation of triple ions and larger complexes accounts for most of solute presence. It is, however, obvious that interpretation of the more concentrated solutions is rather arbitrary, depending on a definition of ionic clusters. Any good model should provide equally good representation, regardless of the applied cluster definition. It is, for instance, perfectly feasible to consider all solute ions paired in the more concentrated solutions as proposed by Anderko and Pitzer,⁶ who correlated available one-phase and two-phase experimental data on NaCl(aq) solutions with an equation of state consisting of a hard sphere reference part and virial expansion perturbation. Their approach was successful for the description of thermodynamic properties of this system at temperatures over 573 K with the exception of dilute solutions, where the presence of free ions is substantial. As noted by Oscarson et al.,⁷ the Anderko and Pitzer model cannot account for any effects due to dissociated chemical species and indeed fails in predicting solute thermodynamic properties at low concentrations. Equilibrium calculations⁸ indicate that this particular concentration range depends largely on temperature and pressure, decreasing from a molality of about 1.5 mol·kg^{−1} at 573 K to some 0.05 mol·kg^{−1} or even lower at supercritical steam conditions. The borders are essentially coincident with concentrations at which appears a maximum in the calculated degree of association of ions to ion pairs.

* To whom correspondence should be addressed. E-mail: josef.sedlbauer@vslib.cz.

It is a common practice in solution chemistry to express solution properties in terms of Gibbs energy, with temperature, pressure, and molality as independent variables. For the chemical potential of solute species, this reads

$$G_i[T, p, m] = G_i^\circ[T, p] + G_i^{\text{ex}}[T, p, m] = G_i^\circ[T, p] + RT \ln(m_i \gamma_i[T, p, m]) \quad (1)$$

where G_i° and G_i^{ex} are the standard and excess chemical potentials, respectively, and γ_i is the solute activity coefficient. The standard state in the unsymmetrical convention is the ideal solution at unit solute concentration (usually molality) referenced to infinite dilution and at the same T and p as the solution of interest. This formulation is very convenient because of its direct connection to chemical and phase equilibrium calculations and because of applying experimentally accessible independent variables. On the other hand, at near-critical conditions Gibbs energy models become impractical for correlation purposes. In this highly compressible region, standard thermodynamic properties are extremely sensitive to small changes in pressure and some of them (e.g., standard molar volume and heat capacity) even diverge at the solvent critical point. The excess part of the model is also affected by this anomalous behavior of the standard state term, because it has to account for the large change in experimental properties upon departing from an infinitely dilute solution to finite concentrations. It was pointed out⁹ that such inherent problems could be avoided by formulating the model in terms of density and temperature rather than pressure and temperature. Recent fundamental equations of state^{6,10–12} operate within such a framework.

The purpose of this work was to provide a description of thermodynamic properties of the dilute NaCl(aq) system in the near-critical range. Accurate representation for this solution is available at temperatures below 573, where the fully dissociated basis was used in connection with the ion-interaction model.² At higher temperatures, the equations of Anderko and Pitzer⁶ can be safely used in the more concentrated region. Therefore, we did not intend to provide a full equation of state with a wide range of applicability: the goal was rather to concentrate on the critical region and low concentrations and to obtain by consistent treatment of experimental data their interpretation in terms of standard and excess properties. We applied a density–temperature-dependent model for both standard and excess properties coupled with a simple model of chemical association. To facilitate practical use of the model, conversion to the Gibbs energy framework is also presented. Because the excess part of the model (given here by the mean spherical approximation, MSA) is only valid in the MacMillan–Mayer (MM) reference state, conversion to the Lewis–Randall (LR) reference is provided at the same time. Data used for correlations in the critical region include the apparent molar volumes,¹³ apparent molar heat capacities,¹⁴ and association constants from several sources. A test comparison with the Pitzer's ion-interaction equations for the excess part of the model was also attempted.

Theory

Gibbs Energy and Its T and p Variations. The central role in the solution thermodynamics is played by the Gibbs energy/1 kg of solution

$$G = \sum_i \mu_i = G^\circ + G^{\text{ex}} \quad (2)$$

where the standard and excess terms have the same meaning as in eq 1. Given this function, it is easy to obtain any other

thermodynamic properties of the solution. The apparent molar volume V^Φ and relative apparent enthalpy L^Φ are

$$V^\Phi = \sum_i \frac{m_i}{m_s} V_i^\circ + \frac{1}{m_s} \left(\frac{\partial G^{\text{ex}}}{\partial p} \right)_{T,m} \quad (3)$$

$$L^\Phi = - \frac{T^2}{m_s} \left(\frac{\partial (G^{\text{ex}}/T)}{\partial T} \right)_{p,m} \quad (4)$$

where m_i is the molality of solute species, m is the total molality $m = \sum m_i$, m_s is stoichiometric molality (number of moles of solute in a kilogram of solution), and V_i° is the standard molar volume. The situation is more complicated in the case of the apparent molar heat capacity C_p^Φ where it is necessary to include also thermal effects associated with the shift of the equilibrium composition during a measurement of the solution heat capacity

$$C_p^\Phi = \sum_i \frac{m_i}{m_s} C_{p,i}^\circ + \left(\frac{\partial L^\Phi}{\partial T} \right)_{p,m} + \frac{1}{m_s} \left(\frac{\partial H_r}{\partial T} \right)_p \quad (5)$$

where $C_{p,i}^\circ$ is the standard molar heat capacity and H_r is the enthalpy due to association reaction. Clearly, the so-called chemical relaxation contribution in eq 5 (the last term on the right side of the equation) is equal to 0 when no chemical reaction occurs in the solution upon a small shift in temperature, such as in completely dissociated strong electrolyte.

Derivatives needed for evaluation of thermodynamic properties might be quite complex, depending on the adopted models for G° and G^{ex} . In some cases, it is, therefore, preferable to calculate them numerically. In addition to Gibbs energy models, preceding equations require the knowledge about concentrations of solute species present at given conditions. This is straightforward when the electrolyte is fully dissociated, but not obvious if association reaction occurs. We shall discuss this topic now, before proceeding to the description of applied G° and G^{ex} models.

Speciation in the Associating System. In a partly associated ionic system, one must account for the presence of ionic clusters. The treatment is presented here for a simple mixture of univalent free ions and uncharged ion pairs, but it can be easily extended to include also higher-order clusters. The first step is evaluation of concentration of different species. In a system with the association reaction of a 1:1 electrolyte



molalities of the present species can be denoted

$$m_C = m_A = m_\pm = (1 - \alpha)m_s \quad (7)$$

$$m_{CA} = \alpha m_s \quad (8)$$

where α is the degree of association obtained by solving the equation for the equilibrium constant

$$K_{\text{as}} = \frac{(1 - \alpha)\gamma_{CA}}{\alpha^2 m_s \gamma_C \gamma_A} \quad (9)$$

with activity coefficients estimated from the excess Gibbs energy model. The association constant is linked to standard chemical potentials of solute species G_i° by the reaction isotherm

$$-RT \ln K_{\text{as}} = \sum_i G_i^\circ \quad (10)$$

To perform speciation calculation, one must, therefore, know the values of G_i° , which are extracted from the model for standard thermodynamic properties.

Standard State Model. Modeling of the standard state thermodynamic properties received much attention in the past decades. Still, the choice is very limited with our particular interest in near-critical thermodynamics. In geochemistry of aqueous electrolytes, main attention has been received by the modified Helgeson–Kirkham–Flowers model.¹⁵ Their equations are given in terms of T and p and do not provide correct near-critical scaling, both features disqualifying for our purpose. Helmholtz energy models such as that of Harvey and Levelt Sengers¹⁶ can only be used with nonelectrolyte solutes. Semi-continuum models^{17,18} were proved to be of insufficient accuracy for the description of standard molar volume and heat capacity. Various engineering approaches^{10–12} emphasize the excess part, resulting in less accurate capturing of the standard state term. We decided to apply the SOCW model proposed recently.¹⁹ This formulation used T and d_1 (density of pure water) as independent variables, thus, alleviating the problem with near-critical anomalies. More importantly, it was shown to be sufficiently versatile and reliable for the correlation of different standard molar properties of ions as well as nonelectrolytes in a wide range of conditions, including the critical region.^{19,20} Description of the SOCW equations was given elsewhere,¹⁹ and only the basic features will be noted here.

Development of the model started with relation between the spatial integral of the standard state solute–solvent direct correlation function C_{12}° and the dimensionless parameter A_{12}° , called the modified Krichevskii parameter

$$1 - C_{12}^\circ = \frac{V_2^\circ}{\kappa_1 RT} = A_{12}^\circ \quad (11)$$

where κ_1 is the solvent compressibility. The A_{12}° function is known to behave smoothly and without anomalies at any conditions²¹ and was, therefore, chosen for correlation. The suggested model for the standard molar volume V_2° consists of three parts. One of them is due to insertion of a point mass into the solvent, the other term reflects the cavity-formation effect of the solute particle, which is supposed to scale with the volume of solvent, and the last part is responsible for solute–solvent interaction

$$V_i^\circ = (1 - z)\kappa_1 RT + d(V_1 - \kappa_1 RT) + \kappa_1 RT d_1 \{a + b[\exp(\vartheta d_1) - 1] + c \exp(\theta/T) + \delta[\exp(\lambda d_1) - 1]\} \quad (12)$$

Universal constants that appear in the model are $v = 0.005 \text{ m}^3 \cdot \text{kg}^{-1}$, $\lambda = -0.01 \text{ m}^3 \cdot \text{kg}^{-1}$, and $\theta = 1500 \text{ K}$; a – d are adjustable parameters, specific for each solute; and z is the charge of a particle ($z = 0$ for neutral molecules, $z \geq 1$ for cations, and $-z \geq 1$ for anions). The $1 - z$ multiplication factor is needed to comply with the hydrogen convention for aqueous ions, which requires $Y_i^\circ(\text{H}^+) = 0$. Using $a = b = c = d = \delta = 0$ for $\text{H}^+(\text{aq})$ would leave the point-mass term ($\kappa_1 RT$) in the equation: it has to be removed by formal assignment of both point-mass terms in a 1:1 electrolyte to the anion. The parameter δ is determined depending on the charge of the solute: for nonelectrolytes with charge equal to 0, $\delta = 0.35a$, for anions, $\delta = -0.645 \text{ m}^3 \cdot \text{kg}^{-1}$, and for cations, $\delta = 0 \text{ m}^3 \cdot \text{kg}^{-1}$. Again, the unsymmetric choice of δ for cations and anions is dictated by the hydrogen convention.

The resulting equation for the standard molar volume is integrated to obtain the Gibbs energy of hydration

$$\Delta_{\text{hyd}} G_i^\circ = RT \ln(p/p_0) + \int_0^p \left(V_i^\circ - \frac{RT}{p} \right) dp + G_i^{\text{corr}} \quad (13)$$

For the hydration process, the integration proceeds from the ideal gas standard state at temperature T and standard pressure $p_0 = 0.1 \text{ MPa}$ to an aqueous solution at T and p . Using the SOCW equation for V_i° , the hydration Gibbs energy is

$$\Delta_{\text{hyd}} G_i^\circ = (1 - z)RT \ln[d_1 RT/p_0] + d\{G_1 - G_1^{\text{ig}} - RT \ln[d_1 RT/(p_0 M_1)]\} + RT\{(a + c \exp(\theta/T) - b - \delta)d_1 + b/\vartheta[\exp(\vartheta d_1) - 1] + \delta/\lambda[\exp(\lambda d_1) - 1]\} + G_i^{\text{corr}} \quad (14)$$

where G_1 is the molar Gibbs energy of water, G_1^{ig} is the same property in the ideal gas standard state, and M_1 is the molar mass of water. The correction function G_i^{corr} was introduced at conditions where the two-phase boundary is crossed in the course of integration from p_0 (the ideal gas standard state) to p , that is, at temperatures lower than the solvent critical temperature T_c . The value of this correction is monotonically decreasing with increasing temperature; it is equal to 0 at the solvent critical temperature T_c and (by definition) equal to 0 at supercritical conditions. We adopted the following functional form of the correction term:

$$G_i^{\text{corr}} = g(T^2 - T_c^2)/2 + (T - T_c)(e - gT_c) + e(\Theta - T_c) \ln \frac{T - \Theta}{T_c - \Theta} - T \left[g(T - T_c) + (e - g\Theta) \frac{T_c}{\Theta} \ln \frac{T}{T_c} + e \frac{\Theta - T_c}{\Theta} \ln \frac{T - \Theta}{T_c - \Theta} \right] \quad (15)$$

where e and g are additional adjustable parameters and $\Theta = 228 \text{ K}$. The standard entropy of hydration is obtained by temperature derivation of $\Delta_{\text{hyd}} G_i^\circ$

$$\Delta_{\text{hyd}} S_i^\circ = - \left(\frac{\partial \Delta_{\text{hyd}} G_i^\circ}{\partial T} \right)_p \quad (16)$$

The standard chemical potential G_i° is calculated by adding the Gibbs energy of solute in the ideal gas standard state to $\Delta_{\text{hyd}} G_i^\circ$

$$G_i^\circ = G_i^{\text{ig}} + \Delta_{\text{hyd}} G_i^\circ \quad (17)$$

It is a common practice to constrain the calculated chemical potentials of the solutes by experimental values of standard thermodynamic properties at some reference conditions, typically $T_r = 298.15 \text{ K}$ and $p_r = 0.1 \text{ MPa}$. After some rearrangement, the previous equation then transforms to

$$G_i^\circ = G_i^{\circ, \text{exp}}[T_r, p_r] - (T - T_r)S_i^{\circ, \text{exp}}[T_r, p_r] + \Delta G_i^{\text{ig}} + \Delta_{\text{hyd}} G_i^\circ[T, p] - (\Delta_{\text{hyd}} G_i^\circ[T_r, p_r] - (T - T_r)\Delta_{\text{hyd}} S_i^\circ[T_r, p_r]) \quad (18)$$

where $G_i^{\circ, \text{exp}}$ and $S_i^{\circ, \text{exp}}$ come from experiment, ΔG_i^{ig} is the change in the ideal gas Gibbs energy between T_r and T , and hydration properties are calculated at the indicated conditions

from eqs 14 and 16. All standard molar thermodynamic properties follow from this fundamental eq 18:

$$H_i^\circ = -T^2 \left(\frac{\partial(G_i^\circ/T)}{\partial T} \right)_p \quad (19)$$

$$C_{p,i}^\circ = -T \left(\frac{\partial^2 G_i^\circ}{\partial T^2} \right)_p \quad (20)$$

$$V_i^\circ = -T^2 \left(\frac{\partial G_i^\circ}{\partial p} \right)_T \quad (21)$$

MSA Model for G^{ex} . MSA and its modifications provide probably the most accurate approach to excess thermodynamic properties currently available. We used its full form for all solutes, but we did not account for interactions among charged and uncharged species. This approximation should be quite fair in dilute solutions, but improvements are possible and will be discussed later. Here, we give the summary of theoretical results relevant to our aims.

Basic Equations of the MSA Framework. Any thermodynamic property in the primitive MSA is composed of two terms, the hard sphere contribution accounting for the short-range repulsive core and long-range electrostatic contribution given by the theory. In the MM reference system, this reads for the excess Helmholtz energy

$$A^{\text{MM}} = A^{\text{HS}} + A^{\text{MSA}} \quad (22)$$

The equation for the electrostatic part of A^{MSA} was given²²

$$A^{\text{MSA}} = -\frac{e^2}{4\pi\epsilon_0\epsilon} \left(\Gamma \sum_i \frac{\rho_i z_i^2}{1 + \Gamma\sigma_i} + \frac{\pi}{2\Delta} \Omega P_n^2 \right) + \frac{\Gamma^3 kT}{3\pi} \quad (23)$$

with

$$4\Gamma^2 = \alpha^2 \sum_i \rho_i \left[\frac{z_i - (\pi/2\Delta) P_n \sigma_i^2}{1 + \Gamma\sigma_i} \right]^2 \quad (24)$$

$$\alpha^2 = -\frac{e^2}{\epsilon_0 \epsilon kT} \quad (25)$$

$$P_n = \frac{1}{\Omega} \sum_i \frac{\rho_i \sigma_i z_i}{1 + \Gamma\sigma_i} \quad (26)$$

$$\Delta = 1 - \frac{\pi}{6} \sum_i \rho_i \sigma_i^3 \quad (27)$$

$$\Omega = 1 + \frac{\pi}{2\Delta} \sum_i \frac{\rho_i \sigma_i^3}{1 + \Gamma\sigma_i} \quad (28)$$

where e is the elementary charge, k is Boltzmann's constant, ϵ_0 and ϵ are dielectric constants of free space and of solution, respectively, σ_i is the diameter of species i , and ρ_i is its number density (this property is connected to molar concentration c_i by $\rho_i = 10^3 c_i N_A$, where N_A is Avogadro's number). The shielding parameter Γ is calculated by an iterative process from the algebraic eq 24. It follows from eq 23 that for nonionic species with zero charge, A^{MSA} is equal to 0. Because there are no data available on dielectric properties of electrolyte solutions at

conditions considered in this study, we applied an approximation in the above formulation that calls for the dielectric constant of the solution independent of composition and equal to that of pure solvent at the same temperature and pressure.

The hard sphere contribution to A^{MM} can be calculated from an appropriate equation of state such as the Carnahan–Starling equation of state²³

$$A^{\text{HS}} = kT\rho \left[\left(\frac{X_2^3}{X_3^2 X_0} - 1 \right) \ln x + \frac{3X_1 X_2}{X_0 x} + \frac{X_2^3}{X_0 X_3 x^2} \right] \quad (29)$$

with

$$X_n = \frac{\pi}{6} \sum_i \rho_i \sigma_i^n \quad (30)$$

$$\rho = \sum_i \rho_i \quad (31)$$

$$x = 1 - X_3 \quad (32)$$

Conversion from MM to LR Variables. To compare with experimental data, A^{MM} needs to be converted from MM reference state to the LR reference system with T , p , and molality m as independent variables. G^{LR} is the excess Gibbs energy per kilogram of solution as in eq 2: superscript LR is used in this section to emphasize the applied reference. The expression for the difference between A^{MM} and G^{LR} was given by Friedman²⁴

$$\begin{aligned} \frac{A^{\text{MM}}[c, T, p]}{cRT} - \frac{G^{\text{LR}}[m, T, p]}{mRT} = \ln \frac{V^*[m, T, p + p_{\text{osm}}]}{V_1[T, p]} + \\ \frac{1}{mRT} \int_p^{p+p_{\text{osm}}} V^*[m, T, p_1] dp_1 - \frac{p_{\text{osm}} V^*[m, T, p + p_{\text{osm}}]}{mRT} \end{aligned} \quad (33)$$

where V_1 is the volume of 1 kg of solvent, p_{osm} is the osmotic pressure, m and c are total concentrations $m = \sum m_i$, $c = \sum c_i$, and V^* is the volume of solution/1 kg of solvent. The concentration variables are connected by

$$m_i = c_i V^*[p + p_{\text{osm}}] \quad (34)$$

An approximation to conversion equations is most often pursued, stating with that p_{osm} is negligible. This assumption leads to great simplification of the conversion term

$$\frac{A^{\text{MM}}}{cRT} - \frac{G^{\text{LR}}}{mRT} = \ln \frac{V^*}{V_1} \quad (35)$$

where V^* is now considered at the experimental pressure p and all other functional variables were omitted for simplicity. V^* is obtained from

$$V^* = \frac{1 + m_s M}{d} \quad (36)$$

with M being molar mass of the solute and d the density of solution, which can be calculated from the apparent molar volume V^Φ and density of pure solvent d_1

$$d = \frac{d_1(1 + m_s M)}{1 + V^\Phi m_s d_1} \quad (37)$$

V^Φ can be assessed from the data or from a model in an iterative procedure. It is, therefore, feasible to apply a complete conversion procedure, because V^* can be calculated at any conditions and integration in eq 33 can be performed numerically. Osmotic pressure required for this calculation comes from the MSA

$$p_{\text{osm}} = \phi^{\text{MM}} kT\rho \quad (38)$$

with $\rho = \sum \rho_i$ and the osmotic coefficient Φ^{MM} is given by

$$\phi^{\text{MM}} = 1 + \phi^{\text{HS}} + \phi^{\text{MSA}} \quad (39)$$

where

$$\phi^{\text{MSA}} = -\frac{\Gamma^3}{3\pi\rho} - \frac{\pi e^2}{2\epsilon_0 \epsilon kT\rho} \left(\frac{P_n}{\Delta}\right)^2 \quad (40)$$

$$\phi^{\text{HS}} = \frac{X_3}{x} + \frac{3X_1X_2}{X_0x^2} + \frac{X_2^3(3-X_3)}{X_0x^3} \quad (41)$$

The analytic expression for the molar activity coefficients of solute species is

$$\ln y_i^{\text{MM}} = \ln y_i^{\text{HS}} + \ln y_i^{\text{MSA}} \quad (42)$$

where

$$\ln y_i^{\text{MSA}} = -\frac{\alpha^2}{4\pi} \left[\frac{\Gamma z_i^2}{1 + \Gamma \sigma_i} - \frac{\pi(P_n)^2}{2(\Delta/\rho)} \right] \quad (43)$$

$$\begin{aligned} \ln y_i^{\text{HS}} = & -\ln x + \sigma_i \frac{3X_2}{x} + \sigma_i^2 \left(\frac{3X_1}{x} + \frac{3X_2^2}{X_3x^2} + 3\frac{X_2}{X_3} \ln x \right) + \\ & \sigma_i^3 \left(\frac{X_0 - X_2^3/X_3^2}{x} + \frac{3X_1X_2 - X_2^3/X_3^2}{x^2} + 2\frac{X_2^3}{X_3x^3} - 2X_2^3/X_3^3 \ln x \right) \end{aligned} \quad (44)$$

It follows from appropriate derivation of eq 33 that the activity coefficient in the LR reference state is given by

$$\ln \gamma_i^{\text{LR}} = \left(\frac{\partial(G^{\text{LR}}/RT)}{\partial m_i} \right)_{T,p,m_j \neq i} = \ln y_i^{\text{MM}} - \ln \frac{V^*[m, T, p + p_{\text{osm}}]}{V_1} \quad (45)$$

Ion-Interaction Model for G^{ex} . The ion-interaction approach¹ adopts an excess Gibbs energy basis and Debye–Hückel limiting law and is, therefore, inappropriate for use in the vicinity of the critical point. This model is, however, very popular and convenient and we wanted to test it with our systems to provide estimates for its application with associating electrolytes at elevated conditions.

The basic Pitzer's equation for G^{ex} has the form of a virial series expansion

$$\frac{G^{\text{ex}}}{RT} = f(I) + \sum_i \sum_j m_i m_j \lambda_{ij}(I) + \dots \quad (46)$$

where $I = \frac{1}{2} \sum_i m_i z_i^2$ is the ionic strength of the solution,

$$f(I) = -\frac{4IA_\Phi}{b} \ln(1 + bI^{1/2}) \quad (47)$$

is the extended Debye–Hückel limiting law term with A_Φ being the Debye–Hückel limiting slope, $b = 1.2 \text{ kg}^{1/2} \cdot \text{mol}^{-1/2}$, and $\lambda_{ij} = \lambda_{ji}$ are binary interaction parameters, depending on I if both i and j species are charged. Ternary and higher-order interactions were not included in the above fundamental equation because they were found only marginally important for the description of thermodynamic properties of highly associated solutions at lower and moderate concentrations²⁵ and we do not expect to use the model in a wider concentration range. The explicit form of G^{ex} for our system with the association reaction of 1:1 electrolyte is

$$\begin{aligned} \frac{G^{\text{ex}}}{RT} = & f(I) + m_\pm^2 (2\lambda_{\text{CA}} + \lambda_{\text{CC}} + \lambda_{\text{AA}}) + \\ & m_\text{N}^2 \lambda_{\text{NN}} + 2m_\pm m_\text{N} (\lambda_{\text{CN}} + \lambda_{\text{AN}}) \end{aligned} \quad (48)$$

The interactions of individual ions are not accessible experimentally, and cumulative parameters were defined as

$$B_\pm = \lambda_{\text{CA}} + \frac{1}{2}\lambda_{\text{CC}} + \frac{1}{2}\lambda_{\text{AA}} \quad (49)$$

$$\lambda_{\pm\text{N}} = \lambda_{\text{CN}} + \lambda_{\text{AN}} \quad (50)$$

Using these parameters, eq 48 becomes

$$\frac{G^{\text{ex}}}{RT} = f(I) + 2m_\pm^2 B_\pm + m_\text{N}^2 \lambda_{\text{NN}} + 2m_\pm m_\text{N} \lambda_{\pm\text{N}} \quad (51)$$

Activity coefficients of the components are obtained by

$$\begin{aligned} \ln \gamma_\pm = & \frac{1}{2} (\ln \gamma_\text{C} + \ln \gamma_\text{A}) = \\ & \frac{1}{2} \left(\frac{\partial f(I)}{\partial I} \right) + 2m_\pm B_\pm + m_\pm^2 \left(\frac{\partial B_\pm}{\partial I} \right) + m_\text{N} \lambda_{\pm\text{N}} = \\ & f^\gamma + m_\pm B^\gamma + m_\text{N} \lambda_{\pm\text{N}} \end{aligned} \quad (52)$$

$$\ln \gamma_\text{N} = 2m_\pm \lambda_{\pm\text{N}} + 2m_\text{N} \lambda_{\text{NN}} \quad (53)$$

where we considered the ion–neutral and neutral–neutral interaction parameters independent of ionic strength and

$$f^\gamma = \frac{1}{2} \left(\frac{\partial f(I)}{\partial I} \right) = -A_\Phi \left[\frac{I^{1/2}}{1 + bI^{1/2}} + \frac{2}{b} \ln(1 + bI^{1/2}) \right] \quad (54)$$

For B_\pm of 1:1 electrolytes, the following formula has been used extensively¹

$$B_\pm = \beta^{(0)} + 2\beta^{(1)} \frac{[1 - (1 + aI^{1/2}) \exp(-aI^{1/2})]}{a^2 I} \quad (55)$$

leading to

$$\begin{aligned} B^\gamma = & 2B_\pm + I \left(\frac{\partial B_\pm}{\partial I} \right) = \\ & 2\beta^{(0)} + \frac{2\beta^{(1)}}{a^2 I} [1 - (1 + aI^{1/2} - \frac{1}{2}a^2 I) \exp(-aI^{1/2})] \end{aligned} \quad (56)$$

where $a = 2.0 \text{ kg}^{1/2} \cdot \text{mol}^{-1/2}$. Other excess properties can be derived analytically, but as in case of the MSA model we used numerical derivations in eqs 3–5.

It should be emphasized that parameters $\beta^{(0)}$, $\beta^{(1)}$, $\lambda_{\pm\text{N}}$, and λ_{NN} depend on temperature and pressure, so they also vary in the course of taking derivatives. Not enough experimental data are possibly available at any particular temperature and pressure

apart from ambient conditions to find all these parameters and their derivatives with reasonable reliability. The only feasible way is to use some model for the interaction parameters, which links together parameters at different T and p . The theoretical basis for correlation of interaction parameters is absent, and the proposed forms are widely different in the literature. Some functions were presented at one reference pressure only.^{26–29} The equations that include both temperature and pressure dependence often could not be used close to the critical point because of a divergence at some temperature in this region.^{2,30} The other functions include many adjustable parameters to be used with confidence for the description of incomplete data on rapidly changing thermodynamic properties at very high temperatures.^{31,32} Oelkers and Helgeson suggested for the virial terms the same temperature and pressure dependence as for their standard (infinite dilution) counterparts, and this assumption was used with good success for the description of several associating systems.³³ However, in this approach some experimental information is required on activity or osmotic coefficients to evaluate integration constants in the functions for interaction parameters. There are virtually no data on activity coefficients or related properties at the conditions of our interest, which makes it difficult to suggest a thermodynamically sound model for interaction parameters. A robust function with little adjustable parameters and no integration constants was, therefore, needed. We supposed that the leading term in the excess Gibbs energy would have a similar functional dependence as the standard state term, which is proportional to the logarithm of solvent density. The simplest choice was, thus,

$$\text{PAR} = a_1 \ln d_1 \quad (57)$$

where the a_1 parameters are adjusted to the data and PAR stands for $\beta^{(0)}$, $\beta^{(1)}$, $\lambda_{\pm\text{N}}$, and λ_{NN} .

Calculations

Experimental Database. The experimental data included in our treatment covered, namely, apparent molar volumes¹³ of NaCl(aq) and apparent molar heat capacities.¹⁴ Both data sets were taken at three isobars $p = 28, 33$, and 38 MPa and at virtually the same concentrations (eight molalities from $m = 0.005 \text{ mol}\cdot\text{kg}^{-1}$ to $m = 1 \text{ mol}\cdot\text{kg}^{-1}$ and at $m = 2 \text{ mol}\cdot\text{kg}^{-1}$, $m = 3 \text{ mol}\cdot\text{kg}^{-1}$). The concentration range was lower at some conditions where phase separation was observed in the measured solutions. Volumetric results extend from $T = 598$ to $T = 725$ K, and C_p^Φ data are from 598 to 691 K (at 38 MPa the measurements were presented only at one temperature, $T = 624$ K). The almost complete compatibility of the experimental ranges proved to be highly beneficial, because data on V^Φ at or close to experimental conditions are needed in the MSA for the MM to LR reference state conversion. We could use for this purpose direct experimental results or interpolate among them. Volumetric data¹³ have been extrapolated for standard state volumes earlier.^{34,35} The ion-interaction approach was used in both cases, and comparable results were obtained for ions, less for the ion pair. Measurements on C_p^Φ by Carter¹⁴ have been still largely unexplored. These results were obtained on a flow calorimeter³⁶ and represent the most complete and accurate set of C_p^Φ measurements on aqueous electrolytes at near-critical conditions. The older results of White et al.³⁷ were not included in this study, because they are available only at one isobar $p = 32$ MPa and molality $m = 0.015 \text{ mol}\cdot\text{kg}^{-1}$ and their uncertainty is expected to be larger because of the older design of the apparatus. Heats of dilution of NaCl(aq) reported by several

authors^{7,38,39} were not used in our correlations: we rather used them for testing extrapolation abilities of our approach.

To separate the standard state term of free ions from that of the ion pair and to constrain further our model, we included some data at the standard state level, obtained by extrapolation to infinite dilution. The included databases (described earlier)¹⁹ on the standard state partial molar volumes and heat capacities of ions cover temperatures from 273 to 623 K and various pressures. Finally, we also used experimental association constants from conductance measurements in the critical region.^{40–45}

Numerical Implementation. Because the regression procedure with our model is not quite obvious, we considered it practical to summarize briefly the key calculation steps. The description applies to the standard state + MSA model; in cases of ion-interaction G^{ex} or MSA with simplified MM to LR conversion, the procedure is more straightforward. Water properties needed in the standard state model were calculated from the equation of state by Hill,⁴⁶ and the dielectric constant was obtained from the formulation of Archer and Wang.⁴⁷ The values of $G_i^{\circ,\text{exp}}[T_r, p_r]$ and $S_i^{\circ,\text{exp}}[T_r, p_r]$ in the standard state eq 18 were from Shock et al.⁴⁸ for the ions and from Sverjensky et al.⁴⁹ for the ion pair. The effective diameters of the ions and ion pair that are required in MSA were taken from Tikanen and Fawcett⁵⁰ and were set equal to $454, 434$, and 472×10^{-12} m for Na^+ , Cl^- , and NaCl^0 , respectively.

1. Data. We included in our fit data on V_i° and $C_{p,i}^\circ$ for $\text{Na}^+ + \text{Cl}^-$ ions at $473 < T < 573$ K along with K_{as} , V^Φ , and C_p^Φ for the associating NaCl(aq) system (see experimental database section). In our simultaneous procedure, experimental results on any other standard or apparent molar properties could be treated at the same time. It had been pointed out earlier¹⁹ that the SOCW standard state model should not be used at solvent densities lower than about 250 kg/m^3 . Data sets applied in correlations, therefore, excluded results at lower densities. Also excluded were results on V^Φ and C_p^Φ at concentrations exceeding the maximum degree of association at given conditions (this cutoff spanned from $m = 1 \text{ mol}\cdot\text{kg}^{-1}$ to $m = 0.05 \text{ mol}\cdot\text{kg}^{-1}$, depending on T and p).

2. Association Constants. These come from eq 10 using standard chemical potentials calculated from the SOCW model. Parameters of this model were at first obtained from a separate correlation of V_i° , $C_{p,i}^\circ$ at $273 < T < 573$ K and of K_{as} data, and in the following iterations they come from the fit of the data set described in step 1. This is the main iteration loop: correlation of all data is repeated until parameters of the standard state model are unchanged (there are no adjustable parameters in our MSA model).

3. Speciation. The degree of association is calculated from eq 9 with activity coefficients coming at first from the extended Debye–Hückel theory. Now having the molalities of the individual species, osmotic pressure stems from eq 38 and MSA activity coefficients from eq 45. These values are used for new speciation calculation, and iteration proceeds until the calculated degrees of association and osmotic pressures remain stable. V^Φ required in the conversion to the LR reference state could be obtained by two different routes: in the first one, we constructed an interpolation function from V^Φ data; the second possibility is to calculate it from the model (eq 3). This second procedure is general; however, it adds much difficulty to the regression, because calculation of V^Φ is again iterative. Therefore, and also because the experimental conditions in Majer et al.¹³ are very close to the region of our interest, we used interpolated experimental results.

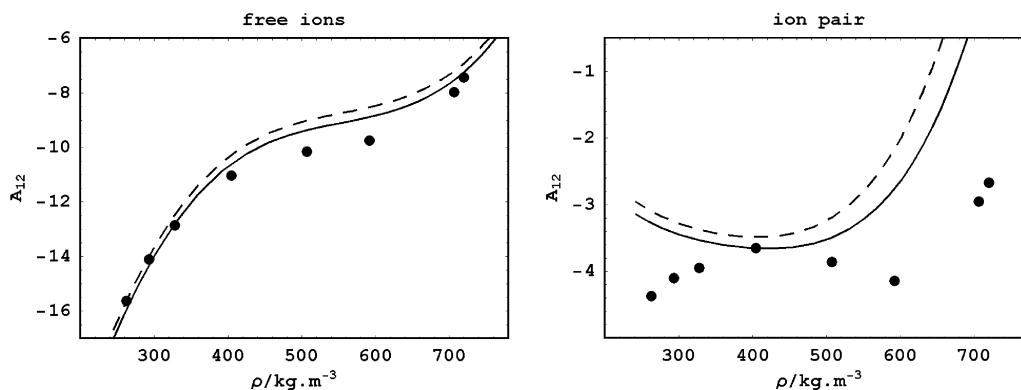


Figure 1. Values of $A_{12}^{\circ} = V_2^{\circ}/(\kappa_1 RT)$ along the $p = 38$ MPa isobar. Full circles, single-point extrapolations;³⁵ full line, SOCW model with parameters from the SOCW + MSA fit; dashed line, SOCW model with parameters from the SOCW + Pitzer fit.

TABLE 1: Parameters of the SOCW Model Obtained from the SOCW + MSA Fit

	a ($\text{m}^3 \cdot \text{kg}^{-1} \cdot \text{mol}^{-1}$)	$b \times 10^4$ ($\text{m}^3 \cdot \text{kg}^{-1} \cdot \text{mol}^{-1}$)	$c \times 10^4$ ($\text{m}^3 \cdot \text{kg}^{-1} \cdot \text{mol}^{-1}$)	d	$e \times 10^3$ ($\text{J} \cdot \text{K}^{-1} \cdot \text{mol}^{-1}$)	g ($\text{J} \cdot \text{K}^{-2} \cdot \text{mol}^{-1}$)
$\text{Na}^+ + \text{Cl}^-$	-0.663 81	0.944 20	0.981 57	1.2446	-0.611 50	1.5474
NaCl^0	-0.006 899 1	3.1973	6.2270	5.0984	-4.3084	10.169

4. $(\partial G/\partial p)_{T,m}$, $[(\partial(G/T)/\partial T)]_{p,m}$, $(\partial L^{\Phi}/\partial T)_{p,m}$, and $(\partial H_r/\partial T)_p$. The partial derivatives needed in eqs 3–5 were obtained by the numerical derivation of the equation for G^{ex} . It should be noted that while molalities m_i are kept constant during all except the last derivation, this is certainly not the case of molarities c_i , which change with the changing density of solution. This effect has to be included in numerical derivations. The chemical relaxation term can be rearranged using the degree of association α

$$\frac{1}{m_s} \left(\frac{\partial H_r}{\partial T} \right)_p = \frac{1}{m_s} \left(\frac{\partial H_r}{\partial \alpha} \right)_p \left(\frac{\partial \alpha}{\partial T} \right)_p = \Delta_r H \left(\frac{\partial \alpha}{\partial T} \right)_p \quad (58)$$

where the molar enthalpy of association reaction is

$$\Delta_r H = H_{\text{CA}}^0 - H_{\text{C}}^0 - H_{\text{A}}^0 + L_{\text{CA}}^{\Phi} - L_{\text{C}}^{\Phi} - L_{\text{A}}^{\Phi} \quad (59)$$

and H_i^0 are standard molar enthalpies of the species, calculated from the SOCW model. Contributions to L^{Φ} for ions and the ion pair are calculated from the model. In most cases, it was found that the contribution of the neutral ion pair to the relative apparent enthalpy is negligible, so L^{Φ} of the system can be safely considered as only due to free ions.

5. *Regression.* The data are regressed, a new set of parameters for the standard state model is obtained, and we proceed back to step 2. Standard state properties are interconnected by thermodynamic relations, eqs 18–21, so one set of mutually compatible parameters is obtained in the fit.

Results

Simultaneous correlations were performed for three models. The standard state term was represented by the SOCW equations in all of them, and the excess term was given by the (i) MSA, (ii) approximate MSA (with simplified MM to LR conversion leading to the G^{ex} fundamental eq 35 rather than eq 33), and (iii) ion-interaction model. Both MSA models lead to essentially the same description of experimental data, and the ion-interaction approach required two or three adjustable parameters ($\beta^{(0)}$, $\beta^{(1)}$, $\lambda_{\pm\text{N}}$) for comparable accuracy of the fit. When attempts were made to extrapolate the results of the models to higher concentrations than those included in the correlation, MSA models provided at least qualitatively correct results, while the ion-interaction predictions were unrealistic. The calculations,

thus, proved the expected inadequacy of the Debye–Hückel + virial expansion approach for near-critical electrolyte solutions. Our interest was, therefore, directed mainly toward the MSA framework. Parameters of the standard state model obtained from regressions with the SOCW + MSA G^{ex} model are given in Table 1.

Figure 1 compares the standard state predictions in terms of the modified Krichevskii parameter A_{12} along the most experimentally explored $p = 38$ MPa isobar. The curves obtained from correlations with both MSA models overlap, and that from the ion-interaction fit is shifted to higher values. Displayed are also results from earlier single-point extrapolations of V^{Φ} data,³⁵ where the estimates of V° were obtained at each T and p separately from correlation of data with the ion-interaction model. Agreement for the ions is good while ion pair predictions are less compatible with the new calculations. It is possible that the bending tendency of single-point results is an artifact due to the extrapolation method in Sedlbauer et al.,³⁵ which only allowed the volumes of the ions to be adjusted on the data because of numerical stability reasons. The volume of the ion pair was obtained from thermodynamic constraint $V_{\text{AC}}^{\circ} - V_{\text{A}}^{\circ} - V_{\text{C}}^{\circ} = -RT(\partial \ln K_{\text{as}}/\partial p)_T$, where an empirical equation for the association constant⁴⁵ was applied and could produce this particular shape. However, it is difficult to claim any conclusive statement about the reliability of the ion pair standard state term. On the other hand, Figure 1 provides reaffirmation of the SOCW model standard state properties of free ions in the near-critical region. To assess its accuracy further, we notice that the data on V_i° , $C_{p,i}^{\circ}$ of free ions at $473 < T < 573$ K that were included in the regressions were described at about their experimental uncertainties ($\sim 4\%$ for V_i° and $\sim 8\%$ for $C_{p,i}^{\circ}$). At higher temperatures, we can compare our predictions with ab initio results on $\Delta_{\text{hyd}}G_i^{\circ}$ of the ions.⁵¹ It can be seen from Figure 2 that the agreement is also good.

Figures 3 and 4 display a series of graphs on the concentration dependence of apparent molar properties V^{Φ} and C_p^{Φ} . Model calculations compare favorably with the data further from the critical point (it should be noted that at supercritical conditions the model curves are in part extrapolations, because some experimental results included in the graphs already correspond to concentrations over maximum association and were not included in the fits). Regression uncertainties for the data in correlations were found to be about 6% for V^{Φ} and 10% for

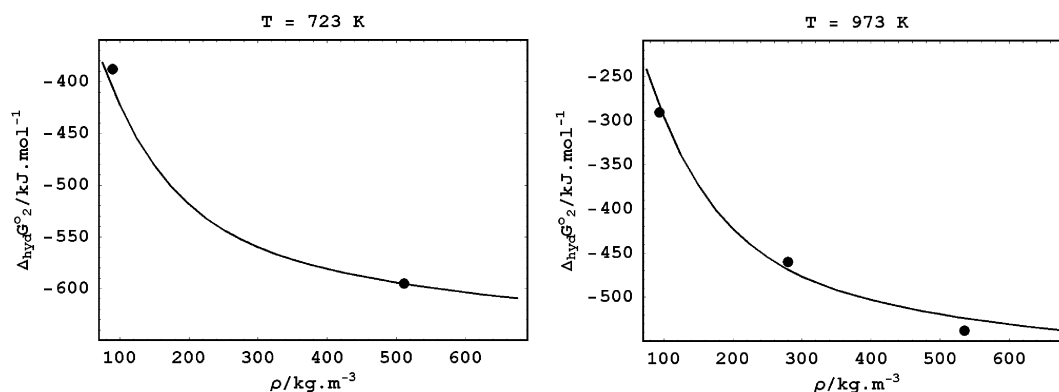


Figure 2. Hydration Gibbs free energies of $\text{Na}^+ + \text{Cl}^-$ ions along the $T = 723 \text{ K}$ and $T = 973 \text{ K}$ isotherms. Full circles, ab initio calculations by Liu et al.;⁵¹ full line, SOCW model with parameters from the SOCW + MSA fit.

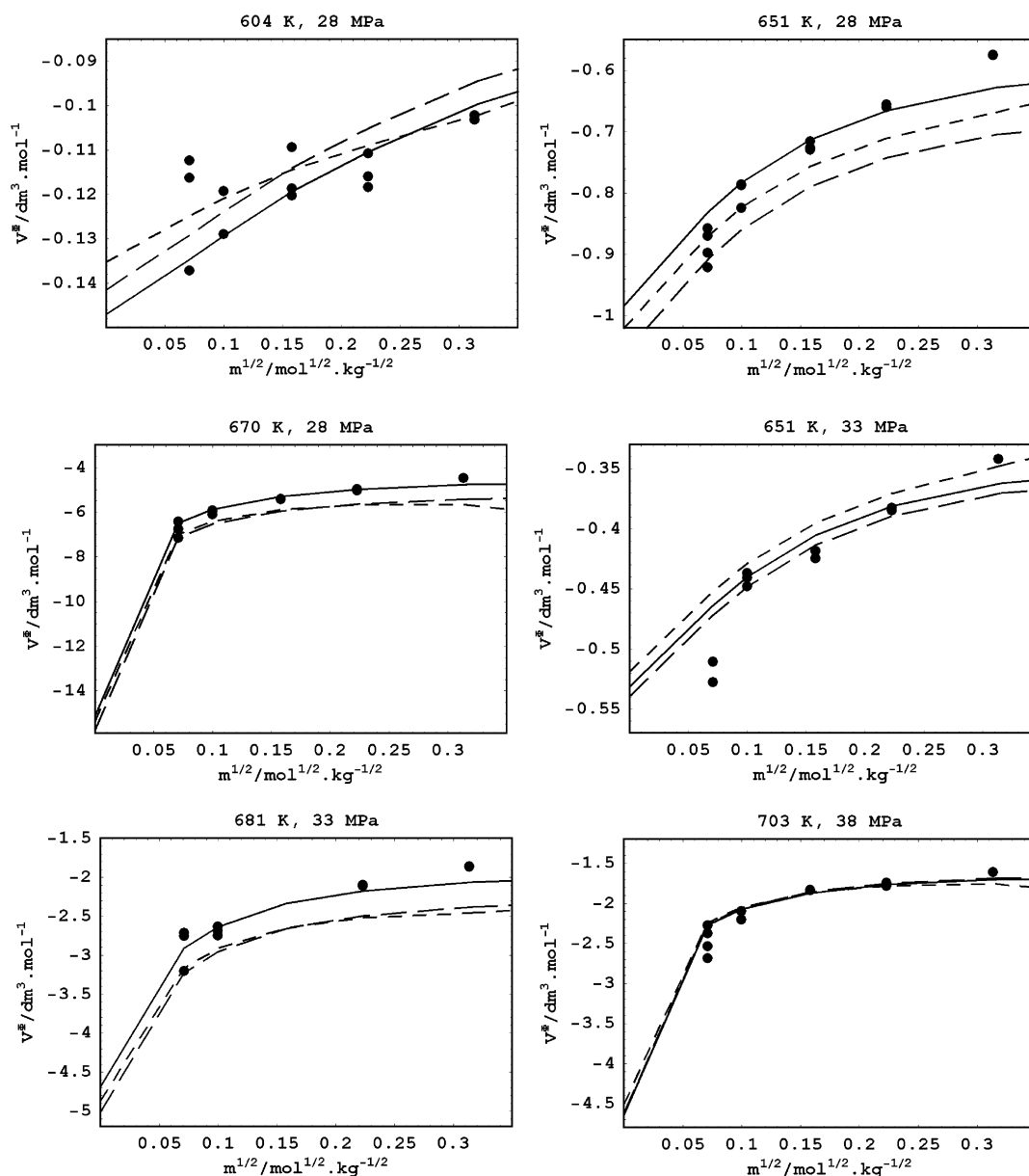


Figure 3. Extrapolations of apparent molar volumes. Full circles, experimental data;¹³ full line, single-point + MSA fit; long-dashed line, SOCW + MSA fit; short-dashed line, SOCW + Pitzer fit.

C_p^Φ , and at least similar uncertainties should be expected for the corresponding standard state properties. There seems to be, however, a systematic deviation at conditions in the immediate vicinity of the critical point. We, therefore, attempted single-point extrapolations with the MSA model and one adjustable

parameter at each $T, p - V^\circ$, or C_p° for ions. For the ion pair, a constraint was applied for the difference $X_{\text{AC}}^\circ - X_{\text{A}}^\circ - X_{\text{C}}^\circ$ in the same way as in Sedlbauer et al.,³⁵ except that the association constant was given by the SOCW model with parameters from Table 1. Description of the data by single-

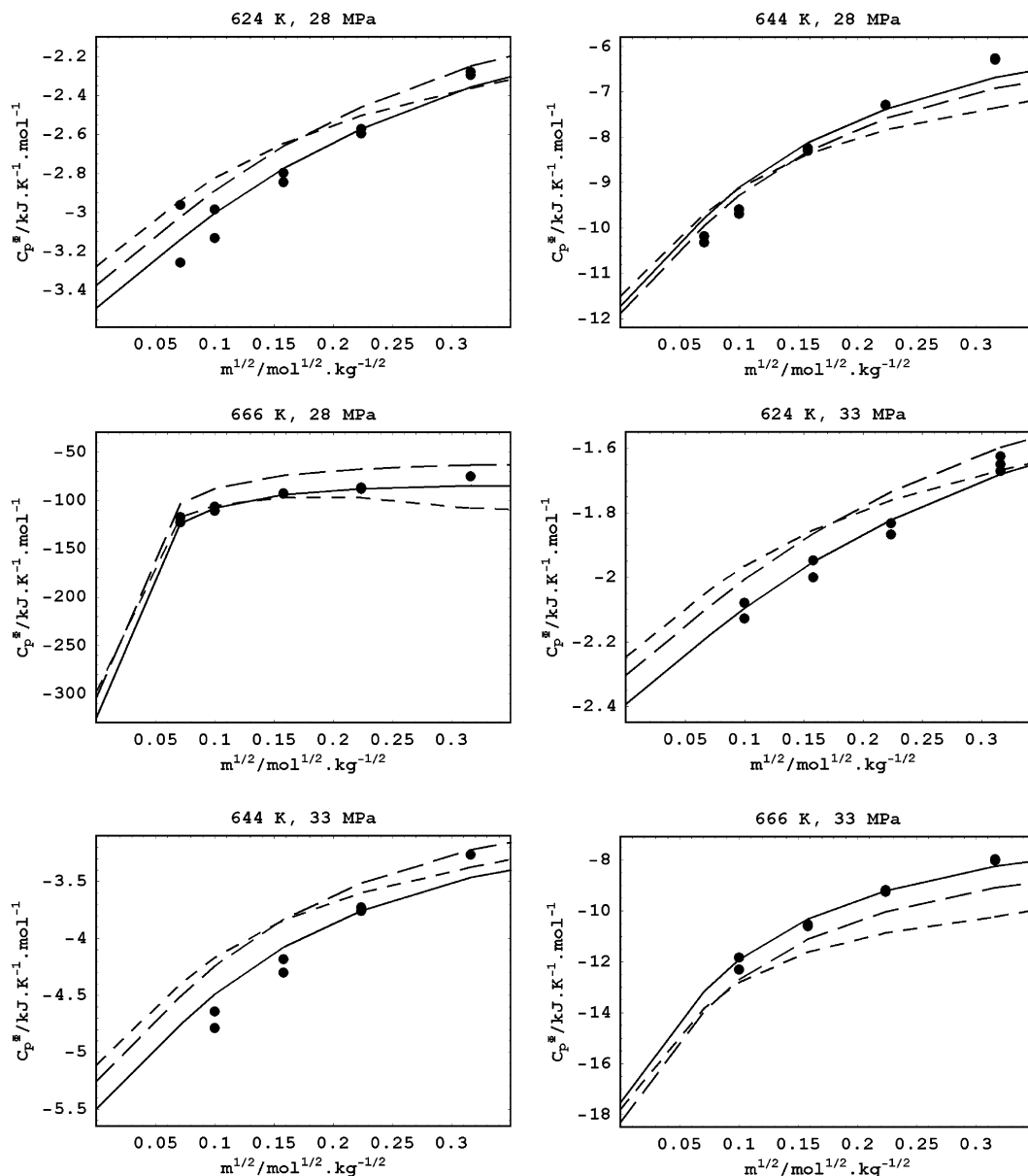


Figure 4. Extrapolations of apparent molar heat capacities. Full circles, experimental data by Carter;¹⁴ full line, single-point + MSA fit; long-dashed line, SOCW + MSA fit; short-dashed line, SOCW + Pitzer fit.

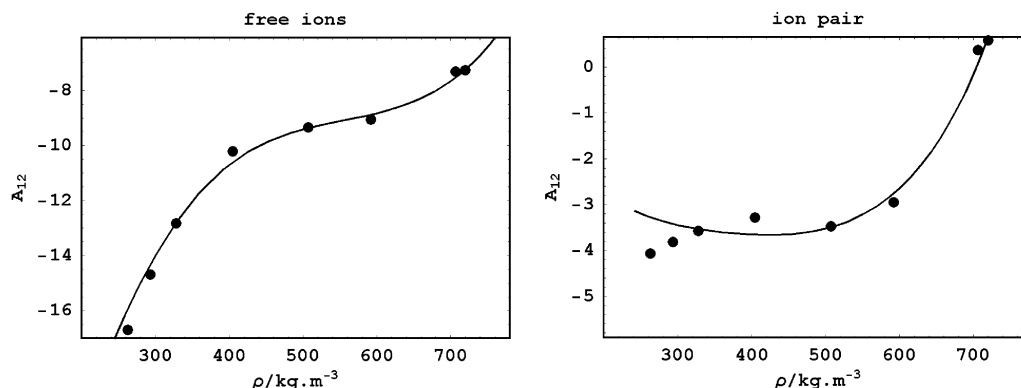


Figure 5. Values of $A_{12}^\circ = V_2^\circ/(\kappa_1 RT)$ along the $p = 38$ MPa isobar. Full circles, single-point extrapolations obtained in this study; full line, SOCW model with parameters from the SOCW + MSA fit.

point extrapolations was markedly improved in the critical region and could be extended to even higher concentrations. The same conclusion is drawn from Figure 5, which is analogous to Figure 1 and displays A_{12} calculated from the model with those from new single-point extrapolations. The agreement is

very good not only for free ions but also for the ion pair. This would mostly suggest that the drift apparent in some Figure 3 and 4 graphs for the SOCW + MSA fit is mainly due to the standard state model that is not flexible enough to capture all peculiarities of the near-critical behavior. On the other hand,

TABLE 2: Standard Molar Volume of Ions and Ion Pairs Obtained from the Single-Point + MSA Extrapolation (Fit), Compared with Values Calculated from the SOCW Model with Parameters from Table 1 (calc) and with Single-Point Extrapolation³⁵ (old)

T (K)	p (MPa)	$V^\circ(\text{Na}^+ + \text{Cl}^-)_{\text{fit}}$ ($\text{cm}^3 \cdot \text{mol}^{-1}$)	$V^\circ(\text{Na}^+ + \text{Cl}^-)_{\text{calc}}$ ($\text{cm}^3 \cdot \text{mol}^{-1}$)	$V^\circ(\text{Na}^+ + \text{Cl}^-)_{\text{old}}$ ($\text{cm}^3 \cdot \text{mol}^{-1}$)	$V^\circ(\text{NaCl}^0)_{\text{fit}}$ ($\text{cm}^3 \cdot \text{mol}^{-1}$)	$V^\circ(\text{NaCl}^0)_{\text{calc}}$ ($\text{cm}^3 \cdot \text{mol}^{-1}$)	$V^\circ(\text{NaCl}^0)_{\text{old}}$ ($\text{cm}^3 \cdot \text{mol}^{-1}$)
604.41	27.4	-147	-144	-148	-22	-19	-58
651.11	28.0	-984	-1061	-1054	-354	-430	-367
665.39	28.0	-7211	-8210	-7103	-1915	-2900	-2072
669.95	28.0	-15098	-15 738	-13 467	-3601	-4264	-4137
673.19	28.0	-16538	-16 183	-14 351	-4016	-3661	-4299
651.11	33.0	-531	-539	-567	-186	-194	-223
668.86	33.0	-1500	-1625	-1654	-511	-637	-560
681.10	33.0	-4687	-5006	-4787	-1346	-1665	-1460
686.55	33.0	-7025	-7218	-6848	-1850	-2033	-2094
691.21	33.0	-8389	-8340	-7889	-2068	-2021	-2318
696.66	33.0	-9114	-8746	-8305	-2187	-1814	-2315
597.45	38.7	-87	-87	-89	7	8	-32
604.42	37.4	-99	-102	-108	5	1	-40
651.10	38.0	-372	-365	-400	-121	-113	-170
673.19	38.0	-921	-923	-1000	-342	-344	-380
691.19	38.0	-2531	-2625	-2732	-813	-905	-904
703.12	38.0	-4636	-4624	-4648	-1290	-1277	-1427
709.55	38.0	-5557	-5411	-5334	-1444	-1294	-1550
716.72	38.0	-6172	-5887	-5774	-1502	-1211	-1616

TABLE 3: Standard Molar Heat Capacity of Ions and Ion Pairs Obtained from Single-Point + MSA Extrapolation (fit), Compared with Values Calculated from the SOCW Model with Parameters from Table 1 (calc)

T (K)	p (MPa)	$C_p^\circ(\text{Na}^+ + \text{Cl}^-)_{\text{fit}}$ ($\text{J} \cdot \text{K}^{-1} \cdot \text{mol}^{-1}$)	$C_p^\circ(\text{Na}^+ + \text{Cl}^-)_{\text{calc}}$ ($\text{J} \cdot \text{K}^{-1} \cdot \text{mol}^{-1}$)	$C_p^\circ(\text{NaCl}^0)_{\text{fit}}$ ($\text{J} \cdot \text{K}^{-1} \cdot \text{mol}^{-1}$)	$C_p^\circ(\text{NaCl}^0)_{\text{calc}}$ ($\text{J} \cdot \text{K}^{-1} \cdot \text{mol}^{-1}$)
598.95	28.0	-1470	-1460	-700	-750
624.08	28.0	-3491	-3380	-1600	-1500
644.50	28.0	-11 930	-11 950	-2430	-2180
655.20	28.0	-36 760	-42 500	-11 110	-16 820
663.18	28.0	-177 100	-203 700	-36 600	-63 600
666.16	28.0	-325 400	-306 600	-86 300	-67 200
671.14	28.0	19 400	90 800	-8100	63 500
673.14	28.0	91 000	124 100	23 100	56 300
676.16	28.0	107 400	116 000	31 000	39 500
682.16	28.0	65 400	65 600	18 000	18 200
598.92	33.0	-1180	-1190	-550	-630
624.11	33.0	-2390	-2300	-1080	-1010
644.40	33.0	-5500	-5250	-2430	-2180
663.17	33.0	-17 530	-18 340	-6150	-7000
651.10	38.0	-1820	-1730	-829	-755

standard state properties obtained by single-point extrapolations suffer from problems typical to this type of treatment: they have large uncertainties and vary with the range of experimental data included in the fit and there is no way to ensure their mutual consistence. V_i° and $C_{p,i}^\circ$ from both single-point + MSA and simultaneous SOCW + MSA regressions are summarized in Tables 2 and 3 at selected experimental conditions. Their comparison also provides an estimate of expected accuracy limits of the standard state properties. Considering all aspects, it is our opinion that regardless of the drawbacks of the current standard state model, the approach referred to here as the SOCW + MSA model should be preferred in cases where several data sets for different properties are available for a given system.

Finally, we compared experimental heats of dilution⁷ with predictions of the SOCW + MSA model. Not all available data could be used for the test, because our way of conversion from the molality to the molarity scale applied an interpolation scheme based on experimental results,¹³ and as a consequence the covered range of conditions is limited by the range of Majer's results with only modest extrapolations possible. It follows from Figure 6 that our calculated values are in good agreement with experiments and provide a substantial improvement compared to the Anderko and Pitzer⁶ predictions, which are also presented in the figure. The modified Anderko and Pitzer model corre-

sponds to an attempt by Oscarson et al.⁷ to couple the original model with an empirical equation for the association constant.⁴⁵

Discussion

The main limitation to this work is probably the accuracy of the applied standard state model. Another uncertainty arises from the range of possible applicability of the Debye–Hückel limiting law and the use of the MSA-based model in the near-critical region. It was argued⁵² that near the critical point the limiting law should be overwhelmed by a critical scaling law. Gruszkiewicz and Wood⁴⁵ did not find evidence of the critical scaling law as close as 2.5 K from the critical temperature, but Myers et al.¹² reported noticeable critical vestiges as far as 100 K from the critical point. However, in their work the calculations were done along the critical isochore where these effects are expected to be much larger compared to cases when the critical point is approached from another direction. At pressures that apply for the data included here (28 MPa and higher), we probably encountered such problems when fitting the results at temperatures to about 10–20 K from T_c . Because we cannot clearly distinguish between the uncertainties produced by critical scaling and those by our models, it is not possible to assess this point conclusively.

We employed in calculations full osmotic pressure conversion between MM and LR reference states and found that this

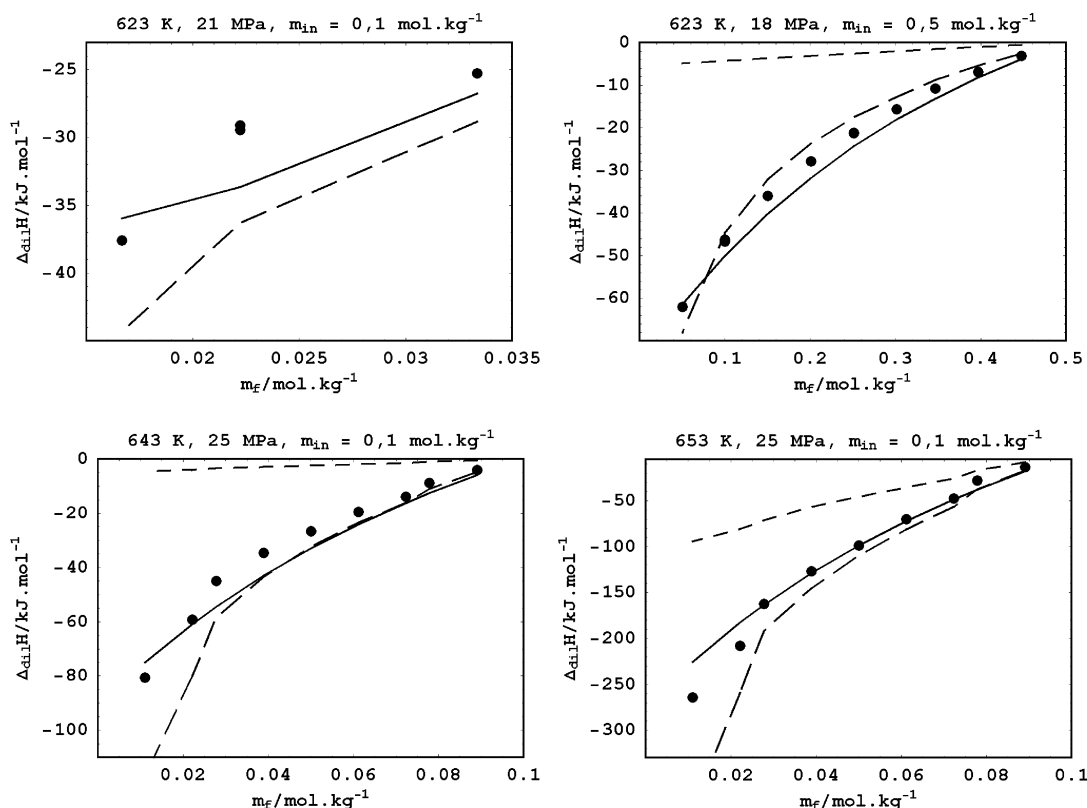


Figure 6. Heats of dilution $\Delta_{dl}H$ versus final solution molality m_f . Full circles, experimental data by Busey et al.³⁸ (623 K, 21 MPa) and by Oscarson et al.⁷ (all other data); full line, SOCW + MSA predictions; long-dashed line, modified Anderko–Pitzer model; short-dashed line, Anderko–Pitzer model.

correction is safely negligible except at very close to the critical point. In the conversion, we were unable to account for the change of the solution dielectric constant with changing concentration of the solute. In the critical region where solution properties change rapidly, an approximation of the concentration-independent solution dielectric constant is problematic. This effect was studied at ambient conditions,^{53,54} and the correction due to this assumption was found small except at moderate and high concentrations (over 2–3 mol·kg⁻¹). In our case, no included experimental results exceed 1 mol·kg⁻¹ in concentration, so we may hope this approximation was still reasonable even at the near-critical conditions.

Improvements of the Model. In principle, the MSA equations were proposed free of adjustable parameters. In this case, only the model for standard state properties can be improved by adjustment to the data. However, it is also possible to introduce adjustable parameters into the MSA model. One choice would be scaling all particle diameters with a uniform scaling factor or by scaling the ions and ion pair separately. Another possibility is addition of the second osmotic coefficients for the interaction of ions of unlikely charge and ions with ion pairs. Apart from these rather empirical adjustments, some changes are possible in the fundamental model equations for both the standard state and excess terms. In the case of the standard state model, the uncertainty is associated namely with the equations for the ion pair that were considered as a nonelectrolyte species. Original development of the model was based on analysis of several nonpolar or weakly polar gases in water and is likely to encounter difficulties when used for an ion pair with a large dipole moment. Because the model is largely empirical, its possible improvements depend on progress in gathering new data on standard thermodynamic properties for very polar solutes. The possible changes to the excess term model account for ion pairing in both the hard sphere and the

electrostatic part of the MSA⁵⁵ or for the dipole character of the ion pair and possibly also of the solvent.⁵⁶

Conclusions

Experimental data on apparent molar volumes, heat capacities, and association constants for dilute NaCl(aq) solutions at near-critical conditions were simultaneously regressed with a new combined model. The standard state part was represented by the SOCW equation, while the excess part of the model came from the MSA. The MSA alone was applied also in single-point extrapolations, separately for each property and set of experimental conditions. The results indicate good performance of both approaches. An important advantage of simultaneous treatment originates from the possibility of using the model for predicting properties and conditions not accessible from experiments. The SOCW + MSA model is, therefore, a promising candidate for consistent treatment of scattered data for thermodynamic properties of associating electrolytes in a wide range of conditions, including very high temperatures and pressures.

Acknowledgment. J.S. was supported by the Grant Agency of the Czech Republic under Contract No. 203/02/0080 and by the Research Plan MSM 254100303. The Department of Energy is acknowledged for support by Grant DEFG01-89ER-14080.

References and Notes

- (1) Pitzer, K. S. *Activity coefficients in electrolyte solutions*; CRC Press: Boca Raton, 1991.
- (2) Archer, D. G. *J. Phys. Chem. Ref. Data* **1992**, 21, 793.
- (3) Rard, J. A.; Archer, D. G. *J. Chem. Eng. Data* **1995**, 40, 170.
- (4) Laria, D.; Corti, H. R.; Fernandez-Prini, R. *J. Chem. Soc., Faraday Trans.* **1990**, 86, 1051.
- (5) Pitzer, K. S.; Schreiber, D. R. *Mol. Phys.* **1987**, 60, 1067.
- (6) Anderko, A.; Pitzer, K. S. *Geochim. Cosmochim. Acta* **1993**, 57, 1657.

- (7) Oscarson, J. L.; Palmer, B. A.; Fuangswasdi, S.; Izatt, R. M. *Ind. Eng. Chem. Res.* **2001**, *40*, 2176.
- (8) Oelkers, E. H.; Helgeson, H. C. *Geochim. Cosmochim. Acta* **1991**, *55*, 1235.
- (9) Levelt Sengers, J. M. H.; Harvey, A. H.; Crovetto, R.; Gallagher, J. S. *Fluid Phase Equilib.* **1992**, *81*, 85.
- (10) Jin, G.; Donohue, M. D. *Ind. Eng. Chem. Res.* **1988**, *27*, 1073.
- (11) Fürst, W.; Renon, H. *AIChE J.* **1993**, *39*, 335.
- (12) Myers, J. A.; Sandler, S. I.; Wood, R. H. *Ind. Eng. Chem. Res.* **2002**, *41*, 3282.
- (13) Majer, V.; Hui, L.; Crovetto, R.; Wood, R. H. *J. Chem. Thermodyn.* **1991**, *23*, 213.
- (14) Carter, R. W. Ph.D. Thesis, University of Delaware, Newark, DE, 1992.
- (15) Tanger, J. C.; Helgeson, H. C. *Am. J. Sci.* **1988**, *288*, 19.
- (16) Harvey, A. H.; Levelt Sengers, J. H. M. *AIChE J.* **1990**, *36*, 539.
- (17) Tremaine, P. R.; Goldman, S. J. *J. Phys. Chem.* **1978**, *82*, 2317.
- (18) Tanger, J. C.; Pitzer, K. S. *J. Phys. Chem.* **1989**, *93*, 4941.
- (19) Sedlbauer, J.; O'Connell, J. P.; Wood, R. H. *Chem. Geol.* **2000**, *163*, 43.
- (20) Sedlbauer, J.; Majer, V. *Eur. J. Mineral.* **2000**, *12*, 1109.
- (21) O'Connell, J. P. *Mol. Phys.* **1971**, *20*, 27.
- (22) Blum, L.; Høye, J. S. *J. Phys. Chem.* **1977**, *81*, 1311.
- (23) Mansoori, G. A.; Carnahan, N. F.; Starling, K. E.; Leland, T. W. *J. Chem. Phys.* **1971**, *54*, 1523.
- (24) Friedman, H. L. *J. Solution Chem.* **1972**, *1*, 387.
- (25) Barta, L.; Bradley, D. J. *J. Solution Chem.* **1983**, *12*, 631.
- (26) Holmes, H. F.; Mesmer, R. E. *J. Solution Chem.* **1983**, *15*, 495.
- (27) de Lima, M. C. P.; Pitzer, K. S. *J. Phys. Chem.* **1983**, *87*, 1242.
- (28) Möller, N. *Geochim. Cosmochim. Acta* **1988**, *52*, 821.
- (29) Phutela, R. C.; Pitzer, K. S. *J. Phys. Chem.* **1986**, *90*, 895.
- (30) Pitzer, K. S.; Peiper, J. C.; Busey, R. H. *J. Phys. Chem. Ref. Data* **1984**, *13*, 1.
- (31) Simonson, J. M.; Holmes, F. H.; Busey, R. H.; Mesmer, R. E.; Archer, D. G.; Wood, R. H. *J. Phys. Chem.* **1990**, *94*, 7675.
- (32) Obsil, M.; Majer, V.; Grolier, J.-P.; Hefter, G. T. *J. Chem. Soc., Faraday Trans.* **1996**, *92*, 4445.
- (33) Oelkers, E. H.; Helgeson, H. C. *Geochim. Cosmochim. Acta* **1990**, *54*, 727.
- (34) Majer, V.; Wood, R. H. *J. Chem. Thermodyn.* **1994**, *26*, 1143.
- (35) Sedlbauer, J.; Yezdimer, E. M.; Wood, R. H. *J. Chem. Thermodyn.* **1998**, *30*, 3.
- (36) Carter, R. W.; Wood, R. H. *J. Chem. Thermodyn.* **1991**, *23*, 1037.
- (37) White, D. E.; Wood, R. H.; Biggerstaff, D. R. *J. Chem. Thermodyn.* **1988**, *20*, 159.
- (38) Busey, R. H.; Holmes, H. F.; Mesmer, R. E. *J. Chem. Thermodyn.* **1984**, *16*, 343.
- (39) Chen, X.; Oscarson, J. L.; Cao, H.; Gillespie, S. E.; Izatt, R. M. *Thermochim. Acta* **1996**, *285*, 11.
- (40) Fogo, J. K.; Benson, S. W. *J. Am. Chem. Soc.* **1954**, *22*, 212.
- (41) Pearson, D.; Copeland, C. S.; Benson, S. W. *J. Am. Chem. Soc.* **1963**, *85*, 1047.
- (42) Quist, A. S.; Marshall, W. L. *J. Phys. Chem.* **1968**, *72*, 684.
- (43) Lukashov, Y. M.; Komissarov, K. B.; Golubev, B. P.; Smirnov, S. N.; Svistunov, E. P. *Teploenergetika* **1975**, *22*, 78.
- (44) Zimmerman, G. H.; Gruszkiewicz, M. S.; Wood, R. H. *J. Phys. Chem.* **1995**, *99*, 11612.
- (45) Gruszkiewicz, M. S.; Wood, R. H. *J. Phys. Chem.* **1997**, *101*, 6549.
- (46) Hill, P. G. *J. Phys. Chem. Ref. Data* **1990**, *19*, 1233.
- (47) Archer, D. G.; Wang, P. J. *J. Phys. Chem. Ref. Data* **1991**, *19*, 371.
- (48) Shock, E. L.; Sassani, D. C.; Willis, M.; Sverjensky, D. A. *Geochim. Cosmochim. Acta* **1997**, *61*, 907.
- (49) Sverjensky, D. A.; Shock, E. L.; Helgeson, H. C. *Geochim. Cosmochim. Acta* **1997**, *61*, 1359.
- (50) Tikanen, A. C.; Fawcett, R. W. *J. Electroanal. Chem.* **1997**, *439*, 107.
- (51) Liu, W. B.; Sakane, S.; Wood, R. H. *J. Phys. Chem. A* **2002**, *106*, 1409.
- (52) Chang, R. F.; Levelt Sengers, J. M. H. *J. Phys. Chem.* **1986**, *90*, 5921.
- (53) Simonin, J.-P.; Blum, L. *J. Chem. Soc., Faraday Trans.* **1996**, *92*, 1533.
- (54) Simonin, J.-P. *J. Phys. Chem. B* **1997**, *101*, 4313.
- (55) Bernard, O.; Blum, L. *J. Chem. Phys.* **1996**, *104*, 4746.
- (56) Carlevaro, C. M.; Blum, L.; Vericat, F. J. *Chem. Phys.* **2003**, *119*, 5198.